Shape Recovery Using Dynamic Subdivision Surfaces

Chhandomay Mandal   Baba C. Vemuri   Hong Qin

Department of Computer & Information Science and Engineering

University of Florida

Gainesville, FL, 32611

Abstract

A new dynamic subdivision surface model is proposed for shape recovery from 3D data sets. The model inherits the attractive properties of the Catmull-Clark subdivision scheme and is set in a physics-based modeling paradigm. Unlike other existing methods, our model does not require a parameterized input mesh to recover shapes of arbitrary topology, allows direct manipulation of the limit surface via application of forces and provides a fast, robust, and hierarchical approach to recover complex shapes from 3D data with very few degrees of freedom (control vertices). We provide an analytic formulation and introduce the physical quantities required to develop the dynamic subdivision surface model which can be deformed by applying forces synthesized from the data. Our experiments demonstrate that this new dynamic model has a promising future in shape recovery from volume and range data sets.

1   Introduction

Recovering shapes of arbitrary topology from large data sets is an important problem in computer vision. A physics-based model which recovers the shape accurately with few degrees of freedom without being restricted to parameterized mesh initialization is a good candidate for the solution. The existing deformable models used to solve this problem can be classified into two categories namely, (1) fixed grid size models [3, 7] using few degrees of freedom for representation at the cost of accuracy of the recovered shape and (2) adaptive grid size models [2, 4, 6] involving large degrees of freedom and computationally expensive ad hoc schemes for accurate shape representation. The hierarchical shape representation using locally adaptive finite elements discussed in [4] can efficiently represent the shape of an object of genus zero with a small number of nodal points. However, this scheme can not be easily extended to cope with arbitrary shapes. The balloon model for describing the shape of complex objects [2] also adapts the mesh surface to local

surface shapes and is purely driven by an applied inflation force towards the object surface when initialized inside the object. This scheme requires a large number of nodal points for representing complex shapes. Moreover, *all the existing models using either a fixed or an adaptive grid size require a parameterized mesh as their input.*

The Catmull-Clark subdivision surface model[1], which is widely used in computer graphics for modeling surfaces of arbitrary topology offer a potential solution, without the aforementioned pitfalls, to the shape recovery problem. This recursive subdivision algorithm generates a smooth surface which is the limit of a sequence of recursively refined polyhedral surfaces based on a user-defined initial control mesh. The Catmull-Clark subdivision surface, defined by an arbitrary non-rectangular mesh, can be reduced to a set of standard B-spline patches in the limit, except at a finite number of *extraordinary* points, where the in-degree of the corresponding vertex in the mesh is not equal to four. *The most interesting property of the Catmull-Clark subdivision surfaces is that the initial control mesh is arbitrary and the underlying smooth limit surface is C^2 continuous*, except at the extraordinary points where it is tangent continuous.

In this paper, we develop a dynamic generalization of Catmull-Clark subdivision surface which inherits the benefits of subdivision surfaces for modeling arbitrary topology and dynamic splines for efficient shape recovery. The model can recover shapes from large range and volume data sets using very few degrees of freedom (control vertices) for its representation. Our model can cope with any arbitrary input mesh, not necessarily parameterized, with an arbitrary number of extraordinary points. The initialized model deforms under the influence of synthesized forces to fit the data set by minimizing its energy. Once the approximate shape is recovered, the model is further subdivided and a better approximation to the input data set is achieved using more degrees of freedom. The process of subdivision after achieving an approximate fit is

continued till a prescribed error criteria for fitting the data points is achieved. It may be noted that the derivation of our dynamic subdivision surface poses a significant technical challenge because of the fact that no closed-form parameterization of the limit surface exists near the extraordinary points. Also, the model involves direct manipulation of the smooth limit surface via application of forces. This is obviously more intuitive than manipulating the control mesh itself especially for computer vision problems involving shape recovery via model fitting. The performance of our proposed modeling scheme in the context of shape recovery is demonstrated via several model fitting experiments with laser range data and magnetic resonance image (MRI) data.

2 Formulation

To develop the dynamic model which treats the smooth limit surface as a function of its control mesh in a hierarchical fashion, we need to update control vertex positions continually at any given level. However, all the vertices introduced through subdivision are obtained as an affine combination of control vertex positions of the initial mesh. Therefore, we can control the dynamic behavior of the limit surface by formulating the dynamic model on the initial mesh itself. To define the limit surface using the vertices of the initial mesh, the enumeration of the bicubic patches in the limit surface is necessary. We now present schemes for assigning the bicubic patches of the limit surface to various faces of the initial mesh.

2.1 Assigning patches to regular faces
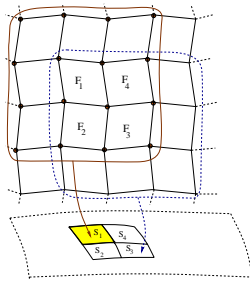
Figure 1: A rectangular mesh and its limit surface consisting of 4 bicubic surface patches.

In Fig.1, a rectangular control mesh is shown along with the bicubic B-spline surface (4 patches) in the limit after an infinite number of subdivision steps. Note that, each of the bicubic patches in the limit surface is defined by a rectangular face with each vertex of degree four, thereby accounting for 16 control points (from its 8 connected neighborhood) needed to
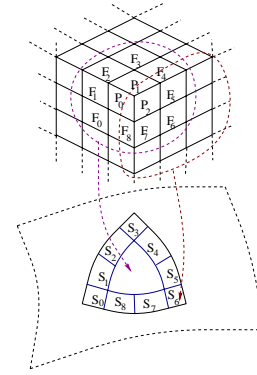
Figure 2: A mesh with an extraordinary point of valence 3 and its limit surface.
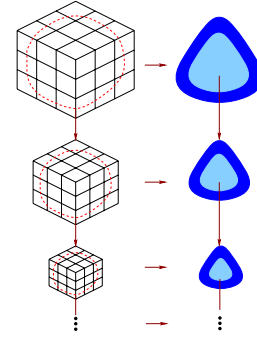
Figure 3: Local subdivision around the extraordinary point and the corresponding patches in the limit surface from different levels of subdivision.

define a bicubic surface patch in the limit. Therefore, for each rectangular face in the initial mesh with a valence of 4 at each vertex, the corresponding bicubic surface patch can be assigned to it in a straight forward way. In Fig.1, the surface patches S_1, S_2, S_3 and S_4 are assigned to face F_1, F_2, F_3 and F_4 respectively. The 16 control points for the patch S_1, corresponding to face F_1, are highlighted in Fig.1.

2.2 Assigning patches to irregular faces

In Fig.2, a mesh containing an extraordinary point of valence 3 and its limit surface are shown. The faces $F_0, F_1, \ldots, F_8$ are assigned to bicubic patches $S_0, S_1, \ldots, S_8$ respectively (as they all have vertices of valence 4) following the aforementioned scheme. However, the central smooth surface enclosed by the patches $S_0, S_1, \ldots, S_8$ consists of infinite number of bicubic patches converging to a point in the limit. We need to develop a recursive way of enumerating these bicubic patches and assigning them to various faces at different levels in order to develop the dynamic subdivision surface model.

The idea of enumerating the bicubic patches corresponding to faces having an extraordinary vertex is shown in Fig.3 where a local subdivision of the mesh enclosed by dotted lines is carried out. Topologically, the resulting local subdivision mesh is exactly the same as the mesh in Fig.2 and hence exactly the same number of bicubic patches can be assigned to its faces with vertices of valence 4. This process of local subdivision and assignment of bicubic patches around an extraordinary point can be carried out recursively and in the limit, the enclosed patch corresponding to faces sharing the extraordinary point will converge to a point. However, there is no need to carry out an infinite number of subdivision steps. This description is for formulation purposes only and the exact implementation will be detailed in a later section.

2.3 Kinematics of the limit surface

In this section we develop the mathematics for the kinematics of the limit surface via illustrative examples and then present the generalized formulas. We start the illustration with a single bicubic B-spline patch which is obtained as the limiting process of the Catmull-Clark subdivision algorithm applied to an initial 4 by 4 rectangular control mesh. Let $\mathbf{s}_p(u, v)$, where $(u, v) \in [0, 1]^2$, denote this bicubic B-spline patch which can be expressed analytically as

$$
\begin{aligned}
\mathbf{s}_p(u, v) &= (x(u, v), y(u, v), z(u, v))^T \\
&= \sum_{i=0}^{3} \sum_{j=0}^{3} \mathbf{d}_{i,j} B_{i,4}(u) B_{j,4}(v)
\end{aligned} \qquad (1)
$$

where $\mathbf{d}_{i,j}$ represents a 3-dimensional position vector at the (i, j)th control point location and $B_{i,4}(u), B_{j,4}(v)$ are the cubic B-spline basis functions. The subscript p on $\mathbf{s}$ denotes the patch under consideration. Expressing Eqn.1 in a generalized coordinate system we have

$$
\mathbf{s}_p = \mathbf{J}_p \mathbf{q} \qquad (2)
$$

where $\mathbf{J}_p$ is the standard Jacobian matrix of a bicubic B-spline patch, and is of size $(3, 48)$. Vector $\mathbf{q}$ is the concatenation of all control points defining a B-spline patch in 3D. Note that in the concatenation of the control points, each control point has an (x, y, z) component. For example, the (x, y, z) components of the control point (i, j) correspond to positions $3k, 3k+1, 3k+2$ - where, $k = 4i + j$ - respectively in the vector $\mathbf{q}$. We can express the entries of $\mathbf{J}_p$ explicitly in the following way: $\mathbf{J}_p(0, k) = \mathbf{J}_p(1, k + 1) = \mathbf{J}_p(2, k + 2) = B_{i,4}(u)B_{j,4}(v)$ and $\mathbf{J}_p(0, k + 1) = \mathbf{J}_p(0, k + 2) = \mathbf{J}_p(1, k) = \mathbf{J}_p(1, k + 2) = \mathbf{J}_p(2, k) = \mathbf{J}_p(2, k + 1) = 0$.

We now define the limit surface $\mathbf{s}$ using the vertices of initial mesh M for any arbitrary topology, assuming all faces are rectangular and no face contains more than one extraordinary point as its vertex (i.e., extraordinary points are isolated). If these assumptions are not satisfied, one or two steps of global subdivision may be required and the resulting mesh can be treated as the initial mesh. Let the number of vertices in the initial mesh M be a, and let l of these be the extraordinary vertices. Let us assume that the number of faces in the initial mesh are b, and that k of these have vertices with valence 4 (henceforth termed a "normal face") and each of the remaining $(b - k)$ faces have one of the l extraordinary vertices (henceforth termed a "special face"). Let $\mathbf{p}$ be the $3a = N$ dimensional vector containing the control vertex positions in 3D. Using the formulations in subsections 2.1 and 2.2, the smooth limit surface can be expressed as

$$
\mathbf{s} = \sum_{i=1}^{k} \mathbf{n}_i + \sum_{j=1}^{l} \mathbf{s}_j \qquad (3)
$$

where $\mathbf{n}_i$ is a single bicubic patch assigned to each of the normal faces and $\mathbf{s}_j$ is a collection of infinite number of bicubic patches corresponding to each of the extraordinary points.

We use the following **notational convention** : the pre-superscript n is used to indicate that these mathematical quantities describe bicubic patch in the limit surface corresponding to normal faces, the pre-superscript s is used to represent a collection of bicubic patches around an extraordinary vertex, the subscript j is used to indicate the j-th extraordinary point, the post-superscript represents the exponent of a mathematical quantity and the level indicator (to represent various levels of subdivision in the local control mesh around an extraordinary vertex) is depicted via subscripts on the curly braces.

It can be shown that

$$
\sum_{i=1}^{k} \mathbf{n}_i = \sum_{i=1}^{k} ({}^{n}\mathbf{J}_i)({}^{n}\mathbf{p}_i) = (\sum_{i=1}^{k} ({}^{n}\mathbf{J}_i)({}^{n}\mathbf{A}_i))\mathbf{p} = ({}^{n}\mathbf{J})\mathbf{p}
$$
$$(4)$$

where ${}^{n}\mathbf{J}_i$ is the Jacobian matrices of size $(3, 48)$, ${}^{n}\mathbf{A}_i$ is a transformation matrix with each row consisting of a single nonzero entry $(= 1)$ and ${}^{n}\mathbf{p}_i$ is the (x,y,z) component concatenation of a subset of control vertices defining the bicubic patch corresponding to the i-th normal face.

The expression for $\mathbf{s}_j$ is derived using the recursive nature of local subdivision around an extraordinary vertex as shown in subsection 2.2. First, $\mathbf{s}_j$ can be expressed as

$$
\mathbf{s}_j = \{{}^{s}\mathbf{J}_j\}_1 \{{}^{s}\mathbf{p}_j\}_1 + \{\mathbf{s}_j\}_1 \qquad (5)
$$

where the first term of Eqn.5 is the generalized coordinate representation of the bicubic B-spline patches corresponding to the normal faces of the new local subdivision mesh obtained after one subdivision step on the local control mesh. $\{\mathbf{s}_j\}_1$ represents the rest of the infinite bicubic B-spline patches surrounding the extraordinary point. The vertices in the newly obtained local subdivision mesh $\{{}^s\mathbf{p}_j\}_1$ can be expressed as a linear combination of a subset of the vertices of the initial mesh M (which will contribute to the local subdivision) following the subdivision rules. We can name this subset of initial control vertices $\{{}^s\mathbf{p}_j\}_0$. Furthermore, there exists a matrix $\{{}^s\mathbf{B}_j\}_1$ of size $(3c, 3d)$, such that $\{{}^s\mathbf{B}_j\}_1\{{}^s\mathbf{p}_j\}_0 = \{{}^s\mathbf{p}_j\}_1$ where $\{{}^s\mathbf{p}_j\}_1$ and $\{{}^s\mathbf{p}_j\}_0$ are vectors of dimension $3c$ and $3d$ respectively. Applying the idea of recursive local subdivision again on $\{\mathbf{s}_j\}_1$, $\mathbf{s}_j$ can be further expanded as

$$\begin{aligned}\mathbf{s}_j &= \{{}^s\mathbf{J}_j\}_1\{{}^s\mathbf{B}_j\}_1\{{}^s\mathbf{p}_j\}_0 \\ &+ \{{}^s\mathbf{J}_j\}_2\{{}^s\mathbf{B}_j\}_2\{{}^s\tilde{\mathbf{p}}_j\}_1 + \{\mathbf{s}_j\}_2\end{aligned} \quad (6)$$

In the above derivation, $\{{}^s\tilde{\mathbf{p}}_j\}_1$ is a vector of dimension $3d$, comprising of a subset of the vertices defining the $3c$ dimensional vector $\{{}^s\mathbf{p}_j\}_1$. Note that, $\{{}^s\tilde{\mathbf{p}}_j\}_1$ has the same structure as $\{{}^s\mathbf{p}_j\}_0$, therefore, there exists a $(3d, 3d)$ matrix $\{{}^s\mathbf{C}_j\}_1$ such that $\{{}^s\mathbf{C}_j\}_1\{{}^s\mathbf{p}_j\}_0 = \{{}^s\tilde{\mathbf{p}}_j\}_1$. Each subdivision of a local mesh with d vertices creates a new local mesh with c vertices which contributes a fixed number of bicubic B-spline patches. So, if we proceed one step further, we obtain

$$\mathbf{s}_j = \{{}^s\mathbf{J}_j\}_1\{{}^s\mathbf{B}_j\}_1\{{}^s\mathbf{p}_j\}_0 + \{{}^s\mathbf{J}_j\}_2\{{}^s\mathbf{B}_j\}_2\{{}^s\mathbf{C}_j\}_1\{{}^s\mathbf{p}_j\}_0$$

$$+\{{}^s\mathbf{J}_j\}_3\{{}^s\mathbf{B}_j\}_3\{{}^s\mathbf{C}_j\}_1^2\{{}^s\mathbf{p}_j\}_0 + \{\mathbf{s}_j\}_3 \quad (7)$$

Because of the intrinsic property of the local recursive subdivision around the extraordinary point, we have $\{{}^s\mathbf{J}_j\}_1 = \{{}^s\mathbf{J}_j\}_2 = \ldots = \{{}^s\mathbf{J}_j\}_n = \ldots = \{{}^s\mathbf{J}_j\}_\infty$. In addition, the subdivision rules remain the same throughout the refinement process, we also have $\{{}^s\mathbf{B}_j\}_1 = \{{}^s\mathbf{B}_j\}_2 = \ldots = \{{}^s\mathbf{B}_j\}_n = \ldots = \{{}^s\mathbf{B}_j\}_\infty$. So, we can further simplify the above equations leading to

$$\mathbf{s}_j = \{{}^s\mathbf{J}_j\}_1\{{}^s\mathbf{B}_j\}_1\{{}^s\mathbf{p}_j\}_0 + \{{}^s\mathbf{J}_j\}_1\{{}^s\mathbf{B}_j\}_1\{{}^s\mathbf{C}_j\}_1\{{}^s\mathbf{p}_j\}_0$$

$$+\{{}^s\mathbf{J}_j\}_1\{{}^s\mathbf{B}_j\}_1\{{}^s\mathbf{C}_j\}_1^2\{{}^s\mathbf{p}_j\}_0 + \ldots$$

$$= \{{}^s\mathbf{J}_j\}_1\{{}^s\mathbf{B}_j\}_1(\sum_{i=0}^{\infty}\{{}^s\mathbf{C}_j\}_1^i)\{{}^s\mathbf{p}_j\}_0 \quad (8)$$

We can rewrite $\mathbf{s}_j$ as

$$\mathbf{s}_j = ({}^s\mathbf{J}_j)({}^s\mathbf{p}_j) \quad (9)$$

where ${}^s\mathbf{J}_j = \{{}^s\mathbf{J}_j\}_1\{{}^s\mathbf{B}_j\}_1(\sum_{i=0}^{\infty}\{{}^s\mathbf{C}_j\}_1^i)$ and ${}^s\mathbf{p}_j = \{{}^s\mathbf{p}_j\}_0$. The idea of local recursive subdivision around an extraordinary point is illustrated in Fig.3. Note that, each vertex position in the subdivided mesh is obtained by an affine combination of some vertices in the previous level and hence any row of $\{{}^s\mathbf{C}_j\}_1$ sums to 1. The largest eigenvalue of such a matrix is 1 and it can be shown that the corresponding infinite series is convergent following a similar approach as in [5]. The rest of the derivation leading to an expression for $\mathbf{s}$ is relatively straight forward. Using the same approach used to derive the Eqn.4, it can be shown that

$$\sum_{j=1}^{l}\mathbf{s}_j = \sum_{j=1}^{l}({}^s\mathbf{J}_j)({}^s\mathbf{p}_j) = (\sum_{j=1}^{l}({}^s\mathbf{J}_j)({}^s\mathbf{A}_j))\mathbf{p} = ({}^s\mathbf{J})\mathbf{p}$$
$$(10)$$

From Eqn.3,4 and 10,

$$\mathbf{s} = ({}^n\mathbf{J})\mathbf{p} + ({}^s\mathbf{J})\mathbf{p} \quad (11)$$

Let $\mathbf{J} = ({}^n\mathbf{J}) + ({}^s\mathbf{J})$, hence

$$\mathbf{s} = \mathbf{J}\mathbf{p} \quad (12)$$

2.4 Dynamics

In an abstract physical system, let $p_i(t)$ be a set of generalized coordinates which are functions of time and are assembled into the vector $\mathbf{p}$. Let $f_i(t)$ be the generalized force assembled into the vector $\mathbf{f}_p$ and acting on p_i. The Lagrangian equation of motion can then be expressed as

$$\mathbf{M}\ddot{\mathbf{p}} + \mathbf{D}\dot{\mathbf{p}} + \mathbf{K}\mathbf{p} = \mathbf{f}_p \quad (13)$$

Let $\mu(u, v)$ be the mass density function of the surface. Then

$$\mathbf{M} = \int\int \mu\mathbf{J}^T\mathbf{J}dudv \quad (14)$$

is an $N \times N$ mass matrix. Similarly the expression for damping matrix is

$$\mathbf{D} = \int\int \gamma\mathbf{J}^T\mathbf{J}dudv \quad (15)$$

where $\gamma(u, v)$ is the damping density.

A *thin-plate-under-tension* energy model is used to compute the elastic potential energy of the dynamic subdivision surface. The corresponding expression for the stiffness matrix $\mathbf{K}$ is

$$\begin{aligned}\mathbf{K} &= \int\int(\alpha_{11}\mathbf{J}_u^T\mathbf{J}_u + \alpha_{22}\mathbf{J}_v^T\mathbf{J}_v + \beta_{11}\mathbf{J}_{uu}^T\mathbf{J}_{uu} \\ &+ \beta_{12}\mathbf{J}_{uv}^T\mathbf{J}_{uv} + \beta_{22}\mathbf{J}_{vv}^T\mathbf{J}_{vv})dudv \quad (16)\end{aligned}$$

where the subscripts on $\mathbf{J}$ denote the parametric partial derivatives. The $\alpha_{ii}(u,v)$ and $\beta_{ij}(u,v)$s are elasticity functions controlling local tension and rigidity in the two parametric coordinate directions.

The generalized force vector $\mathbf{f}_p$ can be obtained through the principle of virtual work done by the applied force distribution $\mathbf{f}(u,v,t)$ and can be expressed as

$$\mathbf{f}_p = \int\int \mathbf{J}^T \mathbf{f}(u,v,t)dudv \qquad (17)$$

3 Finite Element Implementation

The evolution of the generalized coordinates for our new dynamic surface model can be determined by the second-order differential equation as given by Eqn.13. An analytical solution of the governing differential equation can not be obtained in general. However, an efficient numerical implementation can be obtained using the finite element method. For the dynamic subdivision surface model, two types of finite elements are considered - normal elements (bicubic patches assigned to the normal faces of the initial mesh) and special elements (collection of infinite number of bicubic patches assigned to each extraordinary vertex of the initial mesh).

Each normal element is a bicubic surface patch and hence defined by 16 vertices (from the 8-connected neighborhood of the corresponding normal face). For a normal element, the mass, damping and stiffness matrices are of size $(16, 16)$ and can be computed exactly by carrying out the necessary integrations analytically. The matrix $\mathbf{J}$ in Eqn.14, 15 and 16 need to be replaced by $\mathbf{J}_p$ (of Eqn.2) for computation of the local $\mathbf{M}, \mathbf{D}$ and $\mathbf{K}$ matrices respectively of the corresponding normal element.

Each special element consists of an infinite number of bicubic patches in the limit. We have already described a recursive enumeration of the bicubic patches of a special element in Section 2.2. Let us now consider an arbitrary bicubic patch of the special element in some level j. The mass matrix $\mathbf{M}_s$ of this patch can be written as

$$\mathbf{M}_s = \mathbf{\Omega}_s^T \mathbf{M}_p \mathbf{\Omega}_s \qquad (18)$$

where $\mathbf{M}_p$ is the normal element mass matrix (scaled by a factor of $\frac{1}{4^j}$ to take into account of the area shrinkage in bicubic patches at higher level of subdivision) and $\mathbf{\Omega}_s$ is the transformation matrix of the control points of that arbitrary patch from the corresponding control points in the initial mesh. The damping and stiffness matrices for the given bicubic patch can be derived in an exactly similar fashion. Now, these mass, damping and stiffness matrices of all the

bicubic patches corresponding to a special element can be assembled to form the mass, damping and stiffness matrices of that special element. As mentioned earlier, the infinite series summation is convergent. However, it has been found that the contribution from bicubic patches in a special element at a higher level of subdivision to the mass, damping and stiffness matrices becomes negligible and in the implementation, the local subdivision is carried out until the contribution is small enough to be ignored.

The force $\mathbf{f}(u,v,t)$ in Eqn.17 represents the net effect of all applied forces. The current implementation supports spring, inflation as well as image-based forces. However other types of forces like repulsion forces, gravitational forces etc. can easily be implemented.

When the model reaches an equilibrium at a particular level of subdivision, the model can be subdivided, if necessary, according to the Catmull-Clark subdivision rules to increase the number of vertices (control points) and a better fit to the data can be achieved. Currently the error of fit criteria is based on distance between the data points and the points on the limit surface where the corresponding springs are attached. However, other types of error criterion can also be defined and used in this context.

4 Results

The proposed dynamic subdivision surface can be used to recover a wide variety of shapes of arbitrary genus. The only constraint being that the limit surface of the initial polygon should be of the same genus. Note that it is much easier to generate the control mesh whose limit surface is of a given genus than creating a parameterized mesh of a surface with specified genus (as needed by the existing physics-based shape recovery schemes). In this section, we illustrate the performance of our model fitting algorithm via experiments on real (range and volume) data. In all the experiments, the special elements are shaded darker to distinguish them from the normal elements; the initialized model had 96 faces and 98 vertices, 8 of them being extraordinary vertices of valence 3. The final fitted model, obtained through one step of subdivision, has a control polygon of 384 faces with 386 vertices. The tolerance level of the error in fit was set to be 1%.

In Fig.4(a) and (d), we demonstrate the model fitting algorithm applied to laser range data acquired from multiple views of a light bulb. Prior to applying our algorithm, the data were transformed into a single reference coordinate system. The model was initialized inside the 1000 range data points on the surface of the bulb. In the next experiment, the shape of an anvil

is recovered from a range data set (Fig.4(b) and (e)). The range data set has 2031 points. It may be noted that the final shape with a very low error tolerance is recovered using very few number of control points in comparison to the number of data points present in the original range data set. In the last experiment, we present the shape extraction of a caudate nucleus (a cortical structure in human brain) from 64 MRI slices, each of size $(256, 256)$. An expert neuroscientist placed points along the boundary of the caudate shape in each of the 64 slices. Fig.4(c) depicts the points in 3D along with the initialized model. Note that points had to be placed on the boundary of the region of interest due to lack of image gradients delineating the caudate from the surrounding tissue in parts of the image. Continuous image based forces as well as spring forces are applied to the model and the model deforms under the influence of these forces until maximum conformation to the boundaries of the desired caudate shape. The fitted model is shown in Fig.4(f).

5 Conclusions

In this paper, a dynamic generalization of the Catmull-Clark subdivision surfaces is presented which is used for efficient shape recovery. The proposed scheme does not require a parameterized input mesh to recover shapes of arbitrary topology unlike other existing methods. It involves direct manipulation of the smooth limit surface via application of forces and provides a fast as well as accurate way of recovering shapes from large range and volume data sets using very few degrees of freedom. We have presented an analytic formulation of the subdivision scheme, incorporated the advantages of free-form deformable models into the subdivision scheme, introduced hierarchical dynamic control, implemented error-based adaptive subdivision and demonstrated the advantages of our model fitting algorithm via experiments. Our current implementation of the dynamic subdivision surface scheme can not however recover crease edges in the data as no additional constraints are imposed. Also, a local subdivision scheme will further enhance the efficiency of the model representation. Our future efforts will be focussed on addressing these issues.

Acknowledgements

(a)   (b)   (c)

(d)   (e)   (f)
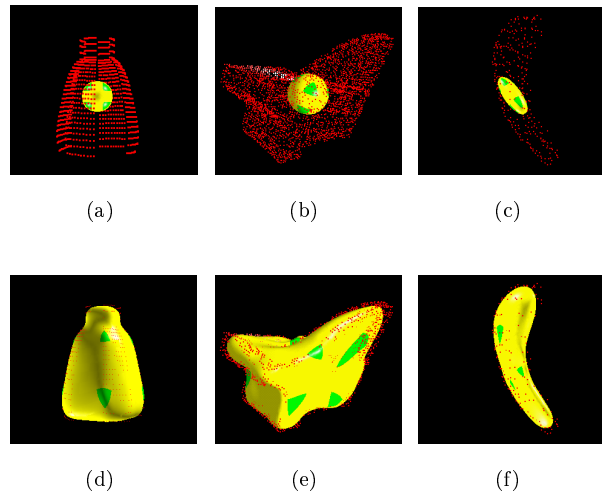
Figure 4: Fitting the dynamic surface model to range data : (a), (b) and (c) are the data along with the superimposed initialized model; (d), (e) and (f) are the corresponding fitted model.

References

[1] E. Catmull and J. Clark. Recursively generated B-spline surfaces on arbitrary topological meshes. *CAD*, 10(6):350 − 355, 1978.

[2] Y. Chen and G. Medioni. Surface description of complex objects from multiple range images. In *CVPR '94*, pp 153 − 158.

[3] L.D. Cohen and I. Cohen. Finite-element methods for active contour models and balloons for 2-d and 3-d images. *PAMI*, 15(11):1131 − 1147, 1993.

[4] E. Koh, D. Metaxas and N. Badler. Hierarchical shape representation using locally adaptive finite elements. In *ECCV '94*, pp 441 − 446.

[5] M. Halstead, M. Kass and T. DeRose. Efficient, fair interpolation using Catmull-Clark surfaces. In *SIGGRAPH '93* , pp 35 − 44.

[6] M. Vasilescu and D. Terzopoulos. Adaptive meshes and shells : Irregular triangulation, discontinuities and hierarchical subdivision. In *CVPR '92*, pp. 829 − 832.

[7] B. C. Vemuri and A. Radisavljevic. Multiresolution stochastic hybrid shape models with fractal priors. *ACM TOG*, 13(2):177 − 207, 1994.